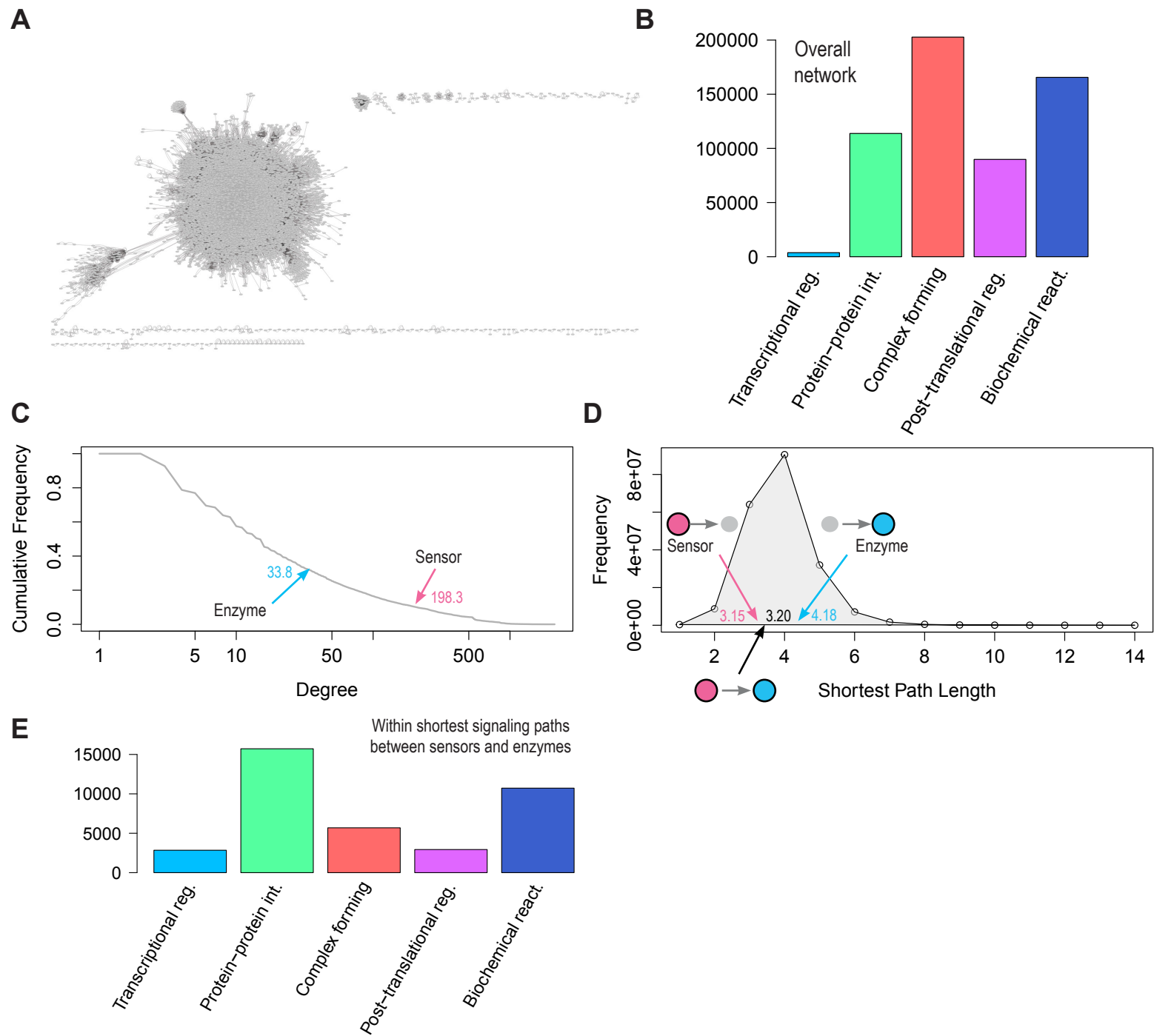
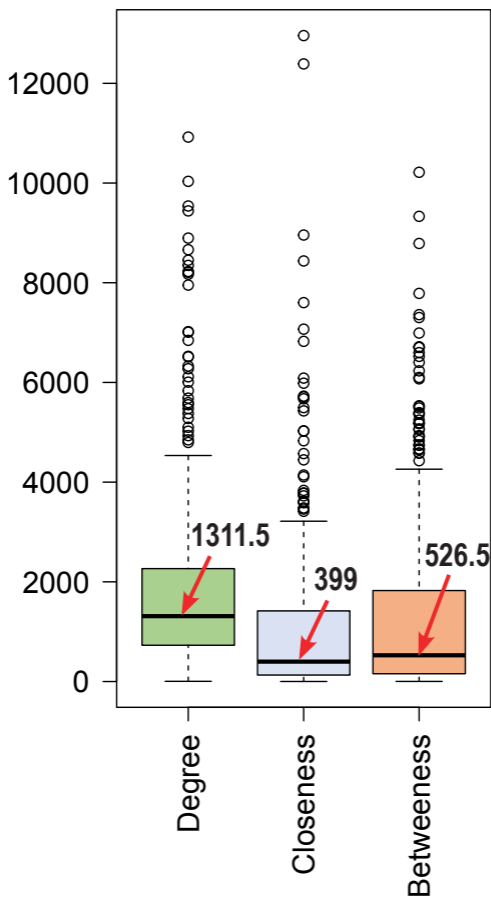


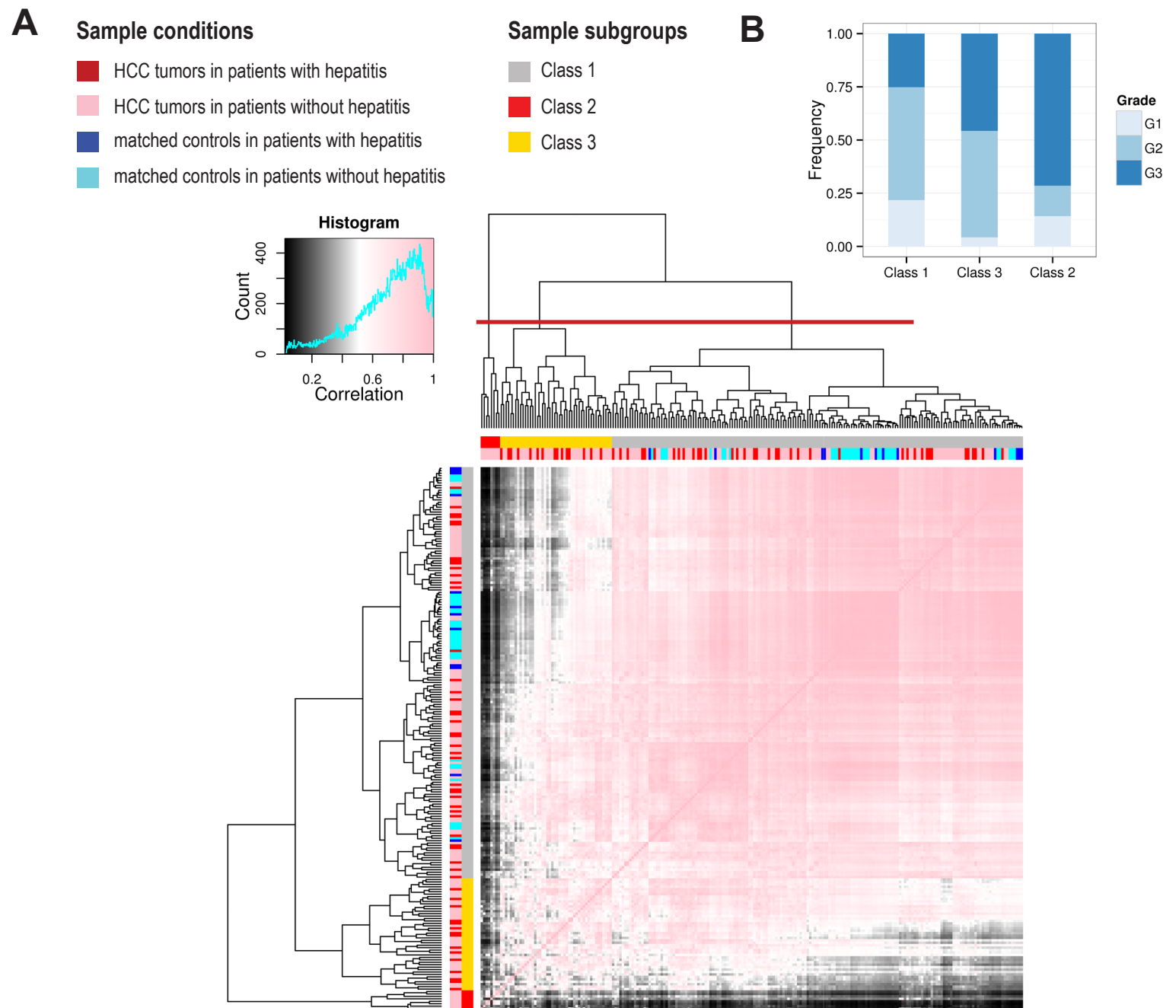
Supplementary Figure S1. An overview of identifying signaling hubs of liver lipid metabolism and investigating their dysregulated expressions in hepatocellular carcinoma (HCC) patients. At the first step, we integrated BioPAX-formatted data of curated signaling pathways (PID, Panther, and Reactome) and large-scale interactomes (PhosphositePlus, HPRD, and CORUM). By Paxtools, Java library (v4.3), we merged those BioPAX-formatted data and extracted all interactions of BioPAX level-3 rules. BioPAX consortium defined diverse bio-molecular interactions through several rules of different levels and we extracted those interactions having level-3 rules, including state-changing interactions (e.g. phosphorylation), transcriptional regulation, physical binding (e.g. protein-protein interaction), protein complex-forming, and biochemical interactions (e.g. complex reassembly). Here we excluded level-3 rules having indirect interactions (i.e. non-physical interactions) like “consecutive catalysis rule”, “controls together rule”, and “metabolic catalysis” or “control rule”. After extracting interactions having BioPAX level-3 rule, we converted those interactions into simple interaction format (SIF), where all biochemical interactions are defined as binary interactions of proteins. At the second step, we collected information about enzymes of 37 lipid metabolic pathways having free fatty acids or eicosanoids as substrates of their reactions from liver-specific genome scale model (GEM), *iHepatocyte2322* and annotated the enzymes of given lipid pathways and lipid sensors, PPAR- α , β/δ , and γ , in the integrated network with SIF format (the third step). Based on this annotated integrated network, we investigated network characteristics, including connectivity and shortest path length. At the fourth step, we identified signaling hubs of each lipid metabolic pathway by bridgeness (i.e. 37 signaling hub sets for lipid metabolic pathways). Based on given enzymes of each lipid pathway and sensors, bridgeness calculated how much a certain gene in the network provides short paths between given sensors and enzymes as many as possible. If some genes are located far apart from shortest paths between sensors and enzymes, bridgeness will score those genes lowly, even though they have high connectivity to other genes in the network. And if sets of sensors and enzymes are changed, bridgeness will give different scores to same genes in the network, which is a distinguishable feature of bridgeness to other general hubness. Thus bridgeness will enable us to identify different sets of signaling hubs according to given enzyme sets. Based on calculated bridgeness scores of all genes in the network, we chose 100 top-scored genes for each lipid metabolic pathway as signaling hubs of given lipid metabolic pathway. Next, based on RNA-seq data of HCC patients from TCGA, obtained via TCGA-Assembler, we examined differential gene expressions between tumors and matched controls of HCC patients (fifth step) by negative binomial tests of DESeq R package (gene-level statistics). As last sixth step, using the p-values of negative binomial tests of individual genes, we calculated pathway-level p-values by comparing log p-values of signaling hubs of given lipid pathway with those of all genes detected in RNA-seq data, as background, by Kolmogorov-Smirnov one-sided tests (pathway-level statistics).



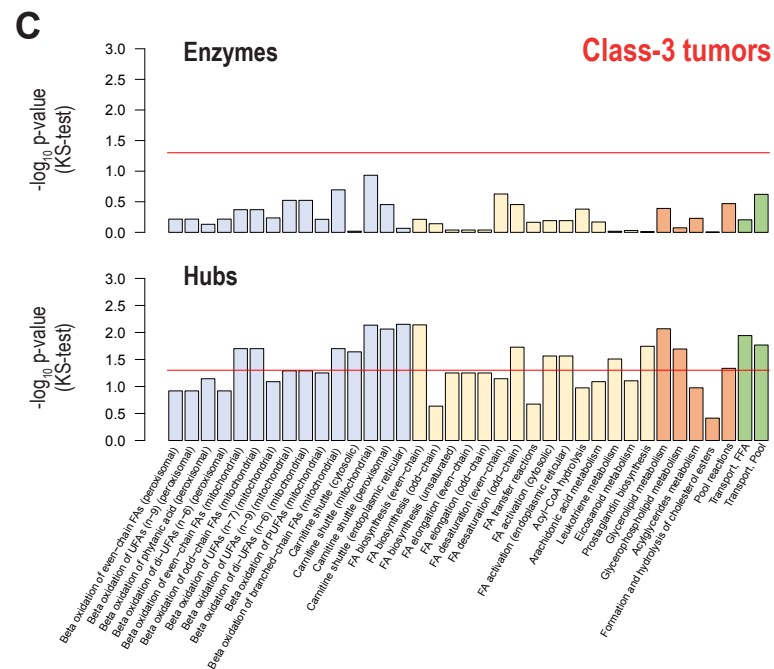
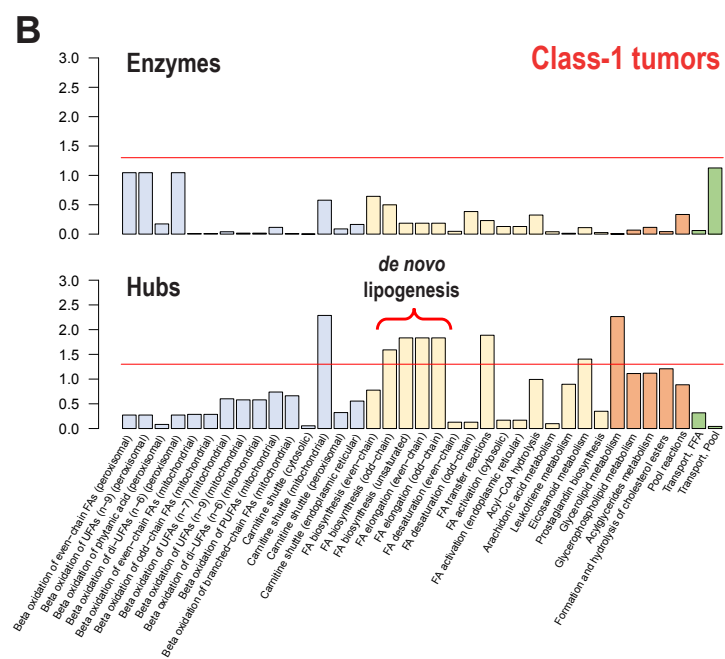
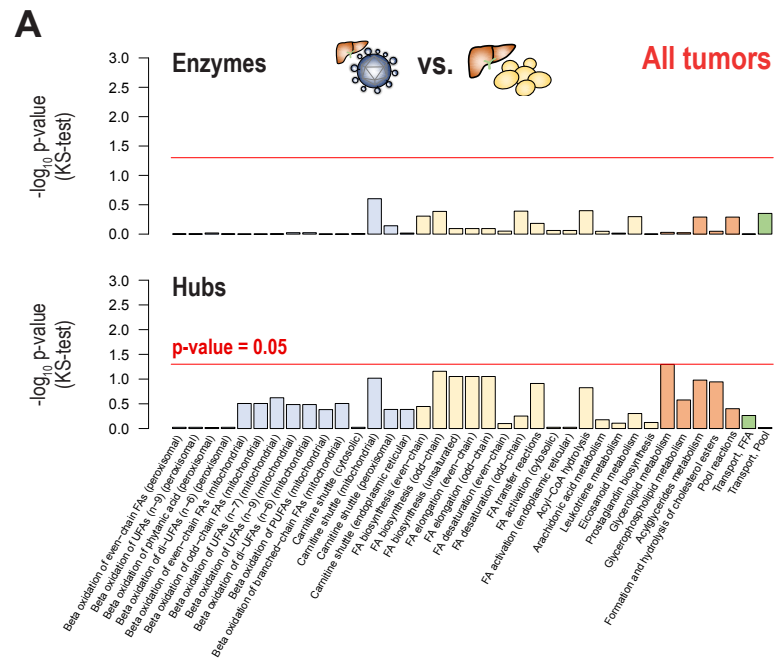
Supplementary Figure S2. The characteristics of an integrated signaling network. This integrated network (A) is established with diverse types of molecular interactions (B), and shows a power-law distribution (C), like other biological networks. Enzymes and sensors do not show high hubness (C), thus locally buried in the network. (D) Signaling paths to enzymes are likely distant (avg. 4.18), even longer than the average of overall network (3.86). However, signaling paths between sensors and enzymes are likely close (avg. 3.20), even shorter than the average. (E) Within shortest signaling paths between sensors and enzymes, types of molecular interactions are also diverse.



Supplementary Figure S3. Rank distributions of identified signaling hub genes in other general hubness measures. We examined ranks of our signaling hub genes in general hubness like degree, closeness, and betweenness. Interestingly, our signaling hub genes showed lowered ranks in other general hubness (even mostly lower than 300th ranks), thus showing their distinctive characteristics to general hubness.



Supplementary Figure S4. RNA-seq samples of HCC patients, shown in a heatmap. A) Sample conditions are colored in both row and column side: HCC tumor samples from patients with viral hepatitis (B and C) (red), HCC tumor samples from patients without viral hepatitis (pink), matched control (normal liver tissue) samples from patients with viral hepatitis (blue), and matched control samples from patients without viral hepatitis (cyan). Interestingly, between patients with viral hepatitis and patients without viral hepatitis, matched control samples are highly correlated (mean Pearson's correlation coefficient (ρ) = 0.93), but HCC tumor samples are not (mean ρ = 0.67). Based on correlation coefficients of gene expressions, we also clustered samples into three subgroups and distinguished with different colors in both row and column side: class 1 (grey), class 2 (red), and class 3 (yellow). Within each sample subgroup, especially class 1 and class 3, we investigated difference of tumor gene expressions between HCC patients with hepatitis and HCC patients without hepatitis. B) We examined tumor characteristics of subgroups that we classified and found differences in tumor grades by each subgroup. Class 1 has many low-grade tumors, whereas class 2 and class 3 have more high-grade tumors.



Supplementary Figure S5. Pathway-level analysis of differential expressions of lipid-regulating genes, signaling hubs and enzymes, in tumors between patients with viral hepatitis and patients without viral hepatitis. Based on the gene-level statistics of the factorial model of Limma R package (Supplementary Table S9), we investigated lipid-regulating genes of given lipid pathway if their differential expressions between tumors and matched controls were distinct in a specific patient group (by KS one-sided test). Using all tumor samples given, we found less differential tumor expressions of signaling hubs (bottom) and enzymes (top) of lipid pathways (A). After clustering tumor samples into three classes, as in Supplementary Figure S4, we re-examined the differential tumor gene expressions between two patient groups at the pathway-level. In class-1 tumors, we found significantly distinct tumor expressions in signaling hubs, in particular of *de novo* lipogenesis, between two patient groups (B). In class-3 tumors, we found significantly distinct tumor expressions of signaling hubs of most lipid pathways between two patient groups (C). Class-2 tumors were not used to examine differential tumor expressions because all of them were only from patients with viral hepatitis. Abbreviations: same as Figure 1